International Journal of
INTELLIGENT SYSTEMS AND APPLICATIONS IN ENGINEERING
ISSN:2147-6799 www.ijisae.org Original Research Paper

A Novel ECNN-Reconstruction of CT Scan Image using Deep Learning

A. V. P. Sarvari, K. Sridevi

Submitted: 04/02/2024 **Revised**: 13/03/2024 **Accepted**: 19/03/2024

Abstract: Medical imaging plays a pivotal role in contemporary healthcare facilities by offering essential assistance for the accurate diagnosis and effective treatment of various disorders. The process of medical image reconstruction holds significant importance within the field of medical imaging, serving as a vital component. Its primary aim is to obtain medical images of superior quality for clinical purposes, while minimizing both the expense and potential risks to patients. Mathematical models have been extensively utilized in the field of medical image reconstruction, as well as in the broader domain of image restoration within computer vision. These models have assumed a significant position in these areas. Historically, mathematical models for image reconstruction have primarily been developed based on human knowledge and hypotheses. The primary objective of medical image reconstruction is to obtain medical images of superior quality for clinical purposes while minimizing the associated costs and risks to patients. Moreover, the process of manual restoration is characterized by a significant time investment, resulting in a substantial accumulation of tasks. This study investigates the utilization of deep learning methodologies to enhance the efficacy of picture reconstruction from fuzzy photos, while concurrently mitigating computing demands. Image reconstruction is achieved by the utilization of an Enhanced Convolutional Neural Network (ECNN), which operates on the principles of Deep Learning. The Fuzzy Granular Filter is employed at the preprocessing stage for the purpose of noise elimination, while the feature map is utilized to enhance the features. The collected features are subsequently fed into the convolutional layers, resulting in an enhancement of quality at each layer. The accuracy of the proposed approach is enhanced in comparison to traditional methods.

Keywords*: Convolutional Neural Network, Deep Learning, Conventional Methods, Features.*

1. Introduction

Researchers have successfully built automatic processing systems for medical images, given their compatibility with computer processing and loading capabilities. During the first period from 1970 to 1990, the field of medical image analysis involved the systematic utilization of mathematical modeling and basic pixel processing techniques to develop composite rule-based models that effectively addressed specific objectives. In the late 1990s, there was a growing prevalence of supervised machine learning approaches in the field of medical image analysis. These approaches involved the construction and training of models using a designated training dataset. The aforementioned pattern recognition technology continues to be well recognized and renowned, serving as the fundamental basis for numerous highly efficient medical imaging systems [1]. The observed transition involves a shift from systems solely built by humans to systems that are trained by computers using example data to extract feature vectors. Researchers in the field of human-computer interaction continue to extract distinctive elements from photos using manually designed models. The subsequent logical step involved enhancing the computational capabilities of computers to efficiently process data that represents relevant qualities for the specific challenge at hand. Numerous deep learning algorithms are founded upon this fundamental principle. Deep learning models, also known as neural networks, consist of multiple layers that transform input data into output representations, facilitating the acquisition of complex features. Currently, convolutional neural networks (CNNs) have gained significant popularity as a prominent class of models for image analysis. In the field of computer vision, deep convolutional networks are

Department of Electrical Electronics and Communication Engineering, GITAM Deemed to be University, Andhra Pradesh, 530045, India.
a.v.p.sarvari@gmail.com

currently regarded as the preferred technique. The utilization of deep learning (DL) techniques in the field of healthcare is now in its nascent stages of advancement.

The process of picture reconstruction is a fundamental component within multiple layers of visual perception. This entails the process of dividing many segments or items [2] through the utilization of visual representations. The process of reconstructing medical images is a fundamental and crucial aspect of medical imaging. Its primary objective is to acquire medical images of superior quality for clinical purposes, while minimizing the associated expenses and potential risks to patients. The process of reconstructing an image can be described as the act of inputting two-dimensional images into a computer system, followed by enhancing or analyzing the image through various transformations to render it in a more constructive and beneficial format for human observation. Deep learning has emerged as a prevalent technique in the fields of computer vision (CV) and image processing, where it is frequently employed for tasks such as picture manipulation, image enhancement, and feature extraction. Medical image analysis, radionics, and computer-aided detection and diagnosis are among areas that have benefited from deep learning (DL) techniques [2, 3]. Deep neural networks have demonstrated significant efficacy across a diverse range of applications, frequently surpassing human performance levels in terms of efficiency.

1.1 Problem Statement

Medical imaging is an essential component in the identification and management of diverse medical ailments, furnishing crucial data for healthcare practitioners. Nevertheless, the integrity of medical images may be considerably diminished due to blurriness resulting from several variables like motion artifacts, constraints imposed by imaging hardware, or inadvertent patient movements. The requirement for unambiguous and correct medical images holds utmost significance in ensuring precise clinical evaluations. Consequently, the issue of medical image blurring emerges as a crucial concern that necessitates attention and resolution.

The challenge lies in creating and implementing efficient deep learning methods for deblurring medical images, which not only enhance the quality of the image but also lower the computational load involved in the process. Because blurry medical images can make it difficult to make an accurate diagnosis, which could result in delayed treatment, incorrect diagnoses, or needless invasive procedures, patients may suffer grave consequences.

1.2 Motivation of the Research Work

Medical imaging plays a pivotal role in contemporary healthcare, offering important insights into the intricate mechanisms of the human body and enabling precise diagnoses and informed decisions for treatment. Nevertheless, although the considerable potential of medical imaging, the integrity of the images is frequently damaged by a range of factors, such as motion artifacts, constraints imposed by the imaging hardware, and concerns connected to the patient. The presence of blurriness in medical images has the potential to obscure crucial features, hence increasing the risk of inaccurate diagnoses and inadequate treatment strategies. These outcomes can significantly impact the quality of patient care. The aforementioned motivation highlights the imperative nature of employing deep learning techniques in the pursuit of medical image deblurring. This study introduces a novel approach, namely the Enhanced Convolutional Neural Network based Deep Learning method, which aims to improve the image quality.

2. Literature Survey

This section will provide an overview of the deep learning models utilized in the domain of medical image analysis as discussed in the examined studies. Machine learning (ML) use statistical methodologies to effectively categorize data into several groups through the process of learning from the available data. There exist three distinct categories of deep learning models, namely conventional, supervised, and unsupervised. In the initial scenario, the system is provided with both the input data and the matching labels associated with the input data. The system establishes a connection between the provided input data and the relevant labels [4]. In the context of unsupervised models, the system is presented with input data that lacks tags or labels. The system visually examines and scans the training data in order to identify and analyze recurring patterns. The result for the unseen data is produced using these maps or patterns.

2.1 Overview of Conventional Image Reconstruction Methods

Generally speaking, image reconstruction is an inverse issue that helps extract the ideal original image from a given subpar version. The process of bringing two-dimensional images into a computer and then manipulating them to make them more useful and aesthetically pleasing for the human eye is known as image reconstruction. In reconstruction (IR), the two main types are analytical reconstruction and repeated reconstruction. Image reconstruction is a fundamental component in the clinical application of magnetic resonance imaging. Converting the obtained k-space data into images that may be clinically understood is the function of image reconstruction. Prior to describing specific image restoration approaches and the signal processing procedures they use, it is crucial to define common tools and vocabulary to characterize the consistency of the reconstructed image. The notion of image quality does not imply a hierarchical comparison between different images. In this context, the term is commonly employed to delineate specific attributes that distinguish one picture reconstruction artifact from another.

2.2 Overview of Deep Learning (DL) Image Reconstruction Methods

In conventional machine learning approaches, the training process involves utilizing human designed characteristics to enable the network to effectively execute the intended task. The manually engineered characteristics are obtained either from raw data or through the utilization of other fundamental machine learning techniques. In the context of deep learning, the features are acquired and taught by computer systems from the data in an automated manner, thus circumventing the arduous process of manually deriving features. Currently, the prevailing models in the field of deep learning are the various iterations of Artificial Neural Networks (ANN). However, it is worth noting that alternative models also exist. One distinguishing characteristic of deep learning (DL) approaches, in comparison to other artificial neural network (ANN) methods, is their emphasis on feature learning. This entails the automatic acquisition of features from data, hence simplifying the process. The integration of feature discovery and task execution occurs concurrently, resulting in mutual enhancement throughout the training phase.

Liu et al., in [5] presents a DL denoising network specifically designed for addressing Poisson noise in photos. The study demonstrates that this network surpasses conventional approaches in terms of performance, with statistically significant enhancements. The network suggested in this study demonstrates a PSNR gain of 0.38dB when subjected to Poisson noise with a peak value of 4. Furthermore, it exhibits even greater gains for more intense noise, with improvements of 1.04dB and 0.68dB observed for peak values of 1 and 2, respectively. Although the computational speed of the approach is 20 times slower compared to the benchmark algorithm, it is possible to enhance the computational speed by modifying the reconstruction stride, while still achieving positive Peak Signal-to-Noise Ratio (PSNR) improvements. The neural network, comprising of six layers, can be considered rather shallow in comparison to contemporary architectures. However, it demonstrates effective performance in Poisson denoising without the need for explicit instruction on noise characteristics. Potential avenues for further research encompass investigating the network's capacity to effectively mitigate various forms of noise, as well as its adaptability to address additional imaging challenges such as deblurring or inpainting.

Chun Yang et al., in [6] investigate the effects of low radiation exposure on the quality of computed tomography (CT) images and conduct a comparative analysis of several reconstruction algorithms. Deep learning image reconstruction (DLIR) at different levels, filtered back projection (FBP), and adaptive statistical iterative reconstruction-Veo (ASiR-V) at varying strengths were used in phantom and clinical trials. The findings of the study on phantom imaging indicate that greater DLIR and ASiR-V strength, in conjunction with higher levels of radiation dosage, were associated with reduced levels of noise. The clinical findings demonstrated that DLIR, specifically at a moderate intensity level (DL-M), exhibited enhanced image quality and noise texture in comparison to FBP and ASiR-V. The DL-M reconstruction method demonstrated superior picture quality and enhanced diagnostic confidence for detecting lesions in low-dose radiation abdominal CT scans, surpassing the performance of alternative reconstruction techniques.

Zuozheng Lian et al., in [7]provide an enhanced U-Net model for picture deblurring that uses a

DMRFC module and a two-dimensional discrete Harr wavelet. Wavelet transforms are employed as an alternative to conventional downsampling and upsampling techniques, resulting in improved image details and less computational complexity. The MRFC module facilitates the dense connection of multireceptive channel blocks, resulting in a reduction of parameters and an enhancement of feature transmission. The suggested methodology exhibits notable reductions in model parameters, decreased running time, and improved visual outcomes in the context of deblurring, as compared to preexisting methodologies. The quantitative assessment conducted on the GOPRO dataset demonstrates a peak signal-to-noise ratio (PSNR) of 30.83 and a structural similarity index (SSIM) of 0.948. These results transcend the performance of alternative deblurring techniques, showing enhanced efficacy and a reduced computational burden.

Rahul N, and Dr. Nagaraj G Cholli, present a work which focuses on identifying undersampled pixels in images and videos through streaming measurements, grouping them into mini-batches, and processing them with dataset inputs. The approach involves aligning multiple image segments with relative displacement on a pixel-by-pixel basis using deep neural networks. This multi-frame design eliminates redundant calculations in aligning several images, improving integration of feature representations and leading to photographs with less noise and higher resolution. The project tackles the challenging task of image reconstruction by simulating degradation processes with blurred and noisy images, aiming to enhance real-world objects. The proposed reconstruction filter, using a suggested truncation approach, retains principal features from the original pixel and offers various forms for directionally adaptive picture restoration using the local covariance matrix.

Akurathi Aravinda et al., [8] investigate the complex task of picture restoration and seek to provide a comprehensive analysis of several strategies employed in this field. Each strategy possesses its own specific methodology for tackling the topic at hand, accompanied by a set of advantages and disadvantages. The choosing of methodology is contingent upon factors such as understanding, specifications, and desired standards of output. The resultant descriptor exhibits qualities of compactness, discriminability, and efficiency. The report presents data that clearly demonstrate a decrease in complexity and an improvement in the ability to comprehend intricate concepts following the implementation of this particular approach.

Kevin De and Yair [9] explores the application of deep learning techniques in the context of altering and rebuilding biomedical pictures obtained using optical microscopy. This study investigates various methodologies aimed at optimizing imaging systems, minimizing expenses, and enhancing the precision of diagnostic assessments in the field of histopathology. The utilization of controlled circumstances in microscopy renders it highly suitable for deep learning purposes, as skilled specialists guarantee meticulous sample preparation and accurate instrument manipulation. Nevertheless, one of the issues that arises in this context pertains to the creation of dynamic datasets and the dependence on data of good quality. The research highlights the considerable promise of deep learning in the field of computational microscopy, namely in facilitating image transformation without the need for approximations of forward models. The proposal recommends the collaborative development of sensing systems and inference algorithms for microscopy applications tailored to specific tasks. This approach has the potential to result in cost-effective imaging techniques capable of high-throughput imaging. The notion of a "intelligent" imaging system, which utilizes past data to make informed decisions, is regarded as a prospective avenue for advancement in the field of microscopic imaging.

Imran Ul Haq in [10] explores the integration of medical imaging with supplementary patient information, such as age and medical history, in order to improve the process of clinical decision-making. The revolution in deep learning is driven by the abundant availability of data, enhanced computational capabilities, and continuous advancements in deep learning algorithms. Despite the obstacles posed by small dataset sizes, there is promising promise in the application of specially created deep learning algorithms for medical imaging. The academic discipline has had a notable increase in scholarly publications, a pattern that is anticipated to persist. As practitioners acquire proficiency, the process of selecting the most appropriate solution method, which may involve end-to-end deep learning methods, integration with alternative approaches, or exclusion of deep

learning components, will be facilitated. In addition to its application in medical imaging, the article posits that deep learning (DL) has the potential to enhance the computational methodologies employed by medical researchers, thereby facilitating the integration of computational medicine into mainstream clinical practice. This advancement is particularly promising due to the involvement of influential disciplines such as computer science, physics, mathematics, and software systems within healthcare institutions.

Yaqub et al., [11] give a comprehensive review paper that examines the latest literature on the application of deep learning techniques in the field of medical imaging, with a specific emphasis on image reconstruction methodologies. The provided resource presents a comprehensive analysis and succinct explanations of the aforementioned techniques. The third section provides a comprehensive overview of commonly employed datasets for magnetic resonance (MR) image reconstruction. This work aims to identify the primary obstacles encountered in the application of deep learning techniques in medical image processing. Additionally, it explores potential strategies and approaches that might be pursued to address these challenges. The literature offered is anticipated to yield significant benefits in the realm of medical imaging applications, augmenting the capacities of artificial algorithms in providing assistance to radiologists.

3. Proposed Work

The objective of medical image reconstruction is to obtain medical images of superior quality for clinical purposes while minimizing expenses. Deep learning models are of significant importance in the field of medical imaging, namely in the domain of image reconstruction. The resulting image obtained from various image modalities may exhibit diminished signal-to-noise ratio (SNR) and contrast-to-noise ratio (CNR), along with the presence of image artifacts.

The objective of medical image deblur is to obtain medical images of superior quality for clinical purposes while minimizing expenses [12]. Deep learning models have a significant impact on the field of medical imaging, specifically in the domain of image deblurring. This study introduces a novel image deblurring model aimed at enhancing image quality and facilitating improved visual understanding. The schematic representation of the planned work's workflow is depicted in Figure 1.

3.1 Pre-Processing

The initial step in the preprocessing of the input image involves the removal of any noise present. This work employs a novel Fuzzy Granular Filtering (FGF) technique to enhance the quality of the input image. Subsequently, an augmented method is employed to further enhance the filtered image.

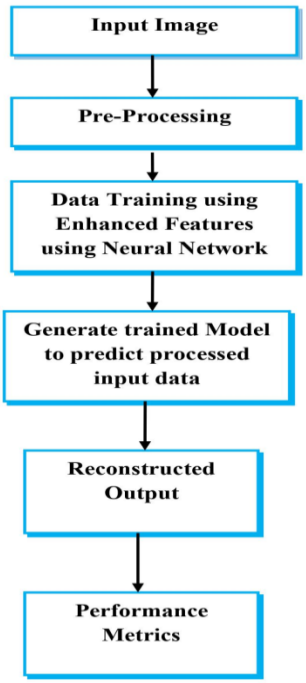

Figure 1: Work Flow of Proposed Methodology

Step 1: Fuzzy Granular filtering

In the context of picture pre-processing, it is important to note that the utilization of external methods may result in the potential loss of information. This paper presents a proposed method for picture pre-processing known as fuzzy granular filtering. A potential classification of filters that may be employed in the processing of CT images is the fuzzy granular filter, which integrates principles from fuzzy logic and granular computing. Fuzzy logic enables the modeling of imprecision and uncertainty, whereas granular computing pertains to the manipulation of data at various levels of granularity [13][14]. The primary objective of these filters is to enhance the quality of images by the reduction of noise, enhancement of edges, and preservation of significant features.

To ascertain the coefficients W_i for the granular filter $W_r(i)$, it is necessary to possess the binary information granule definition within each image window around the pixel x_n that is now being analyzed. In order to achieve the intended objective, it is imperative to take into account the granular function inside two distinct subranges, namely the left and right sides of x_i. There are three potential possibilities that can be considered.

$$W_r(i) = \begin{cases} W_r^p(i), & Max_{i<n}\, W_i > Max_{i>n}\, W_i \\ W_r^q(i), & Max_{i<n}\, W_i > Max_{i>n}\, W_i \\ W_r^t(i), & Max_{i<n}\, W_i > Max_{i>n}\, W_i \end{cases} \quad (1)$$

Where,

$$W_r^p(i) = \begin{cases} 1, & p \le x_i \le x_n \\ 0, & otherwise \end{cases} \quad (2)$$

$$W_r^q(i) = \begin{cases} 1, & x_n \le x_i \le q \\ 0, & otherwise \end{cases} \quad (3)$$

$$W_r^t(i) = \begin{cases} 1, & p \le x_i \le q \\ 0, & otherwise \end{cases} \quad (4)$$

In all equations, p and q denotes the extreme information granule range values

The fuzzy granular approach necessitates the redefinition of the function in a manner that assigns a continuous membership value to the information granule. The initial stage involves normalizing the granular function to a range between 0 and 1.

$$W_N(i) = \frac{W_i}{max_{0 \le i \le M-1}\, W_i} \quad (5)$$

The function, as described by equations (1) to (4), accurately represents the measure of similarity between each given sample and the value of x_n. The creation of the fuzzy information granule results in the generation of values that approach 1, indicating a high degree of similarity to the information granule. The methodology for deriving the fuzzy weights function is outlined in Figure 2. As the samples deviate more from x_n, the weights function $w_f(i)$ decreases in magnitude. The control parameter α has an impact on both the range of the information granule (as determined by the values of p and q) and the rate at which the weight function decays.

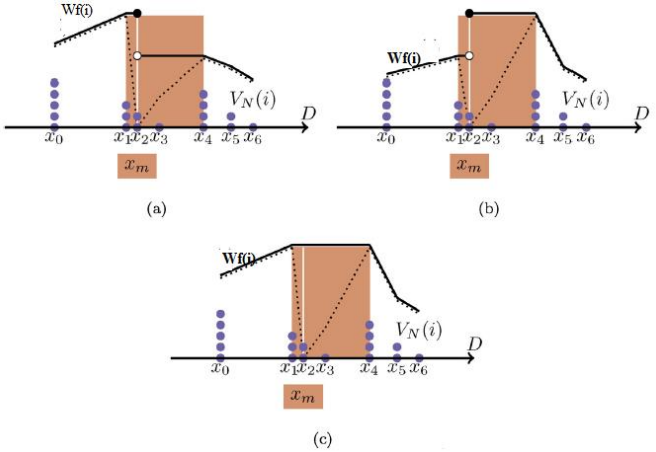

Figure 2: Weighted functions of fuzzy granular function in all p, q and t cases

To apply this filtering initially need to define the member ship function. A fuzzy membership

function that assigns membership values to pixel intensities. This can be attain by using the equation (6)

$$\mu(x) = \max(0,1) - \frac{|x-0.5|}{fuzziness\_factor} \quad (6)$$

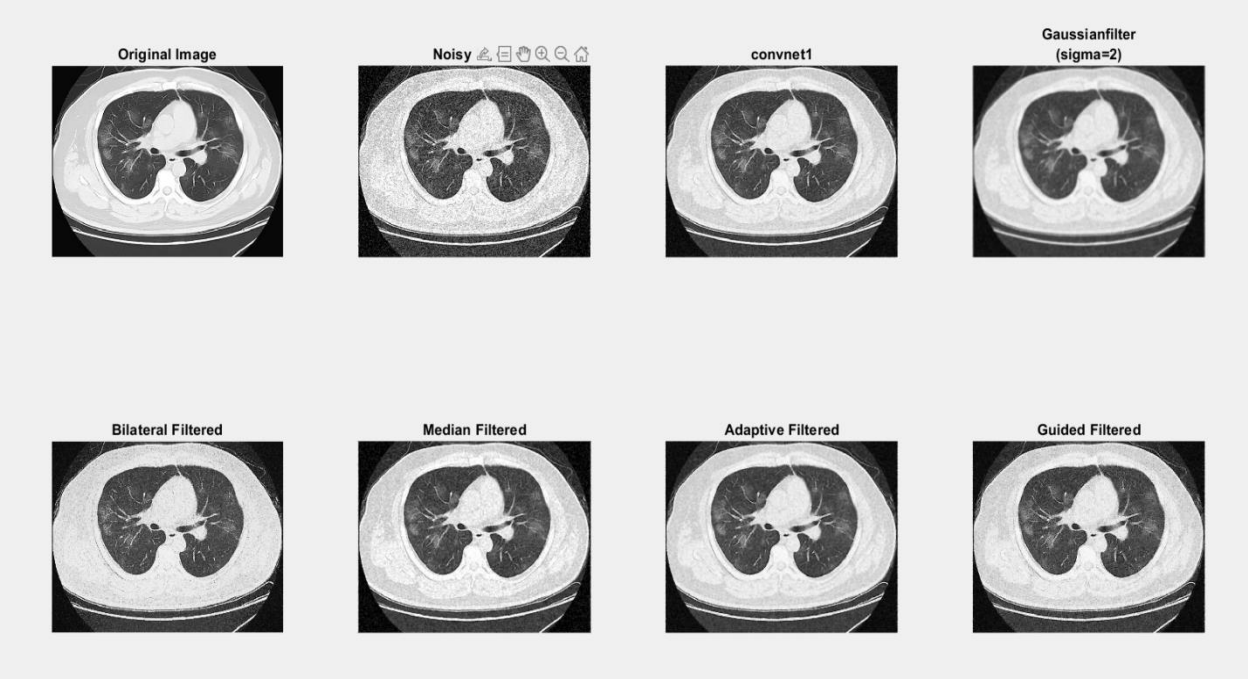

Figure 3: Original and filtered image

Algorithm 1: image pre-processing using Fuzzy Granular Filtering

Input: CT Scan image in 2D array, neighborhood_size, fuzziness_factor

Output: Fuzzy granular filtered CT scan image

Step 1: Define Fuzzy Membership function by using Equation (6)

Step 2: Initialize Filtered Image by creating an empty array in 2D

Step 3: Performa the iteration through all the pixels in input image

$$\boldsymbol{for\ i\ in(0, height);}$$

$$\boldsymbol{for\ j\ in(0, width)\ ;}$$

Step 4: Extract the local neighborhood around the pixel by using Equation (7)

$$neighborhood = inputimage\left[i - \frac{neighborhood\ size}{2} : i + \frac{neighborhood\ size}{2} + 1, j - \frac{neighborhood\ size}{2} : j + \frac{neighborhood\ size}{2} + j\right].flatten() \quad (7)$$

Step 5: Apply the fuzzy granular filter to the pixel using the membership values from the neighborhood by using Equation (8)

$$filtered\ image[i,j] = \max\left(\mu(x) for\ x\ in\ neighborhood\right) \quad (8)$$

3.2 Contrast Enhancement using Novel Enhanced Convolutional Neural Network (ECNN)

Feature extraction refers to the systematic procedure of carefully choosing, altering, and converting unprocessed data into distinct attributes that possess the potential to be effectively utilized within the realm of deep learning. To optimize the performance of deep learning models on novel tasks, it may be important to develop and train enhanced features[15][16]. The attribute in question may pertain to the hue of an entity or the auditory qualities of an individual's vocalization. Feature engineering is the process of transforming raw data observations into meaningful features through the utilization of deep learning methodologies.

A deep learning system typically comprises a sequential combination of a Convolutional Neural Network (CNN). The objective of Convolutional Neural Networks (CNNs) is to autonomously produce features that can be easily separated. Before the advent of deep convolutional networks, the majority of inputs for vision-based tasks were of a different nature. The convolutional neural

network (CNN) component of a deep learning system is trained to iteratively generate a progressively refined set of features across the various levels of the CNN. Put differently, the final output of the convolutional neural network (CNN) layer is the most enhanced and polished collection of characteristics. Extensive research has been conducted to demonstrate that the feature spaces produced by a Convolutional Neural Network (CNN) exhibit characteristics of manifold mappings [18]. The CNN component of deep convolutional networks functions as a feature extractor. The augmentation of separable features generated by the Convolutional Neural Network (CNN) is anticipated to result in an improvement in network performance.

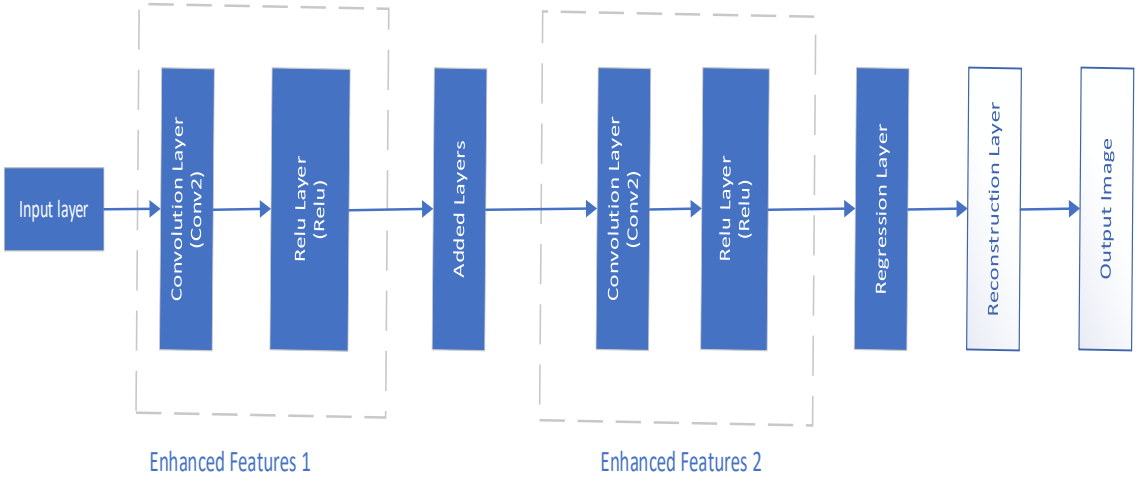

Figure 4: Layered Architecture of CNN

Added Enhanced Layers

Neural networks are a category of computational models that are constructed using multiple layers. The system consists of an input layer and an output layer. The architecture described imposes a constraint on the perceptron, limiting its ability to address classification issues that are linearly separable, meaning those that can be divided by a solitary straight line [19][20]. However, numerous classification problems encountered in real-world scenarios exhibit non-linear characteristics. In order to address this challenge, the concept of the single-layer perceptron was extended by incorporating additional intermediate layers positioned between the input and output layers. The intermediate layers in question are sometimes denoted as "hidden" layers, whereas the augmented network is commonly referred to as a "multi-layer perceptron". The figure 4 illustrates the representation of a layered architecture.

Every individual unit within a concealed layer does a computational operation on the weighted inputs it receives, resulting in an output that is subsequently utilized as an input for the subsequent layer. The subsequent layer in question may consist of either another concealed layer or the output layer, which generates the probabilities associated with each label. The inclusion of a hidden layer within a neural network architecture provides us with the capability to effectively address intricate mathematical problems.

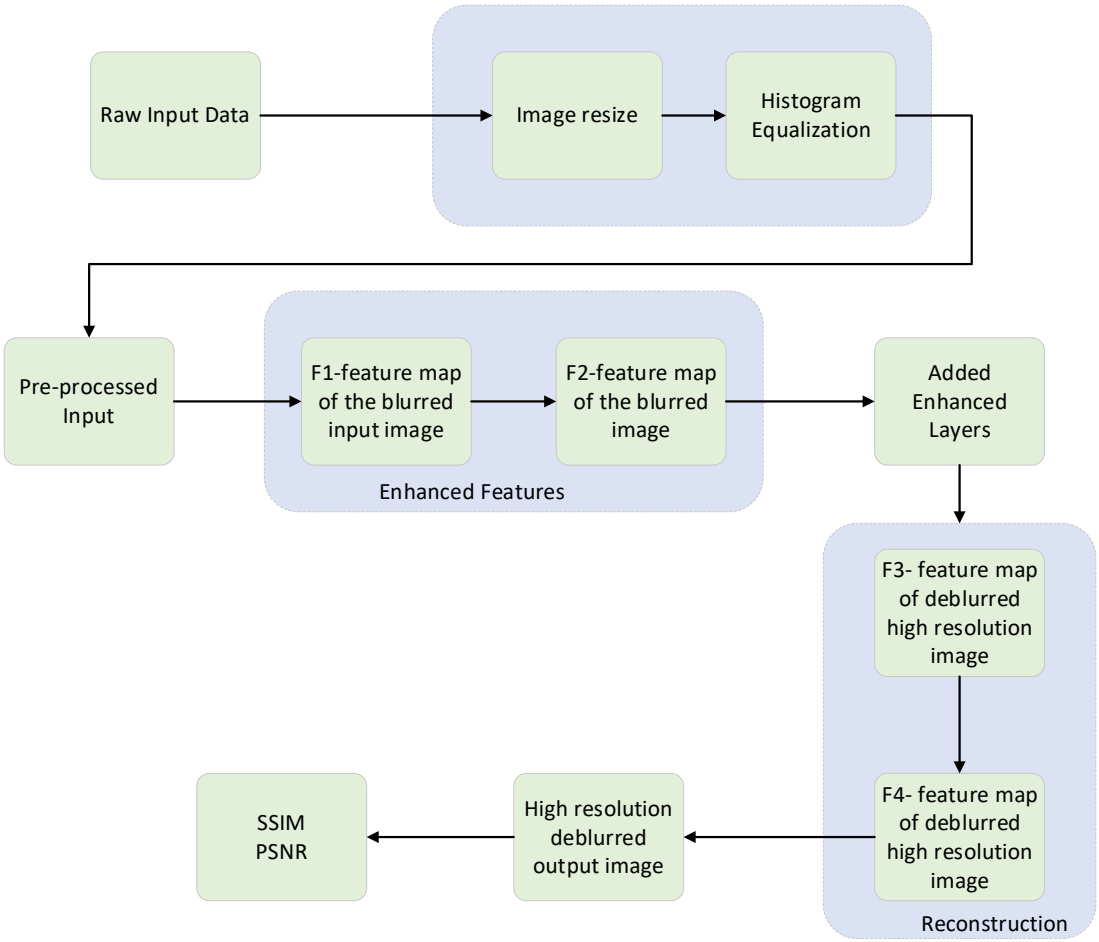

Figure 5: Block Diagram of Proposed Work

The network described in this study accepts a blurred low-resolution image x as its input and generates a deblurred high-resolution reconstruction F(x) directly. The architectural design comprises of four convolutional layers, together with a concatenation layer, as illustrated in Figure 5 of the provided block diagram.

Layer Architecture of ECNN

i. Input Layer

The initial layer, known as the input layer, is responsible for calculating the low-level features. It consists of 32-feature maps, sometimes referred to as filters, each with a filter size of 9 x 9.

Dimension: $HXWXC$, H is height, W is weight and C is the number of channels.

Activation: Linear

ii. Convolutional Layer 1

The second layer is a component that enhances the features extracted from the first layer. It consists of 32-feature maps with filters.

Filters: N_1 filters with size $K_1\ X\ K_1$. In this we can adjust the K_1 based on the complexity.

Stride: S_1

Padding: P_1

Activation: ReLU

The convolutional layer can be detailed by using Equation (9)

$$Z^{[1]} = W^{[1]} * I + b^{[1]} \quad (9)$$

Here $W^{[1]}$ is the convolutional kernel. $b^{[1]}$ is the bias, * denotes the convolutional operation and $Z^{[1]}$ is the output feature map.

iii. Convolutional Layer 2

The third layer combines the characteristics extracted from the preceding two layers, resulting in a combined vector that encompasses both low-level and enhanced features [22]. The layer in this is comprised of either 64-feature maps or 32-feature maps, depending on the specific operation that determines the merging method.

Filters: N_2 filters with size $K_2\ X\ K_2$. In this we can adjust the K_2 based on the complexity.

Stride: S_2

Padding: P_2

Activation: ReLU

The activation function in each layer is obtained by using Equation (10). The ReLU introduces the non-linearity function to the layer.

$$A^{[1]} = ReLU\left(Z^{[1]}\right) \quad (10)$$

iv. Max Pooling Layer

Max pooling reduces the spatial dimensions of the feature map.

In a Max Pooling Layer, the goal is to down-sample the spatial dimensions of the input tensor by selecting the maximum value from a group of neighboring pixels. This helps in reducing the spatial resolution while retaining the most important features.

Pool size: P_{size1}

Stride:$P_{stride1}$

$$P^{[1]} = MaxPooling(A^{[1]}) \quad (11)$$

v. Flatten Layer

Converts the output to a 1D vector. It Takes the multi-dimensional input pixel and flattens it into a one-dimensional vector. It Unrolls or reshapes the image pixel and removing all dimensions except for one.

if X is the input tensor and Y is the output of the Flatten layer

$$Y = flatten(X) \quad (11)$$

$$Y = flatten\left(X^{[final]}\right) \quad (12)$$

The flattened vector F is obtained from the final pooling layer.

vi. Fully Connected Layer 1

A fully connected layer combines features from the flattened vector.

Let X be the input vector to the fully connected layer, and W be the weight matrix, b the bias vector, and Y the output vector.

The input vector **X** has *M* elements, and the fully connected layer has *N* neurons. The weight matrix **W** has dimensions *N*×*M*, and the bias vector **b** has dimensions *N*×1.

The output Y is calculated by using Equation (13)

$$Y = W.X + b \quad (13)$$

Interms of individual image pixel elements the output is calculated by using equation (14)

$$Y_i = \sum_{j=1}^{M} W_{i,j}.X_j + b_i \quad (14)$$

- *Yi* is the *i*-th element of the output vector **Y**.
- *Wij is the weight of the connection between the i-th neuron in the fully connected layer and the j-th element of the input vector X.*
- *Xj is the j-th element of the input vector X.*
- *bi is the i*-th element of the bias vector **b**.

vii. Output Layer

In this proposed ECNN architecture, the Dense layer with a single neuron and linear activation is used as the output layer for regression. The model is then compiled with an appropriate optimizer and loss function for regression tasks.

In enhanced CNN is designed for a classification task, you can use the Softmax activation function in the output layer. Assuming you have C classes, the output layer would typically have C neurons, and the activation function applied is the Softmax.

$$Y_i = \frac{e^{x_i}}{\sum_{j=1}^{C} e^{x_j}} \quad (15)$$

The operations encompassed in this set are summation, maximum, subtraction, averaging, multiplication, and concatenation. With the exception of the final operation, all of these operations require inputs of the same size and provide outputs of the same form. The process of concatenation enables the combination of inputs with varying sizes [23]. The concatenation procedure has been observed to have the highest level of performance based on empirical evidence. The subsequent layer executes the mapping of second order. The ultimate layer is responsible for the reconstruction of the high-resolution output image.

Table 1: Details of Layers in ECNN

Patch	Kernel	Stride	Layer	Dimension
8 X 8	NA	NA	Concatenation	512
8 X 8	8 X 8	NA	Fully Connected	256
8 X 8	8 X 8	NA	Fully Connected	2
8 X 8	3 X 3	2	Max Pooling	128
16 X 16	3 X 3	1	Convolution 1	64

16 X 16	3 X 3	1	Convolution 2	128
8 X 8	3 X 3	1	Convolution 3	256

Weighted Average on Layer

During the execution of the weighted average step, the coefficients included in the weight map can be conceptualized as the diffusion rule, which determines the proportion of each corresponding contrast value in the source picture. The probability that is ultimately determined serves as the weight value in the weight map. A greater likelihood is attributed to the pixels in the High Contrast (HC) CXR image or the Low Contrast (LC) CXR pixels that possess a higher amount of contrast information. A weight map is generated, which is of the same size as the input picture pair, by utilizing the pre-trained Convolutional Neural Network (CNN) model. In the weight map σ, pixels that appear brighter indicate a value in proximity to 1, whereas pixels that appear darker indicate a value in proximity to 0.

As an example, if the weight map assigns a value of 0.97 to a pixel at coordinates (i,j), it indicates that the LC CXR pixel contributes 97% of the weight at that location, while the HC CXR pixel contributes 3% of the weight. The computation of the averaged pixel value is performed by.

$$Output(i,j) = L_C CXR\ (m,n) * (1 - \sigma(\mathrm{i,j})) \quad (6)$$

The variables "output (i, j)", "LC CXR (i,j)", "HC CXR (i,j)", and "σ (i,j)" represent the pixel value of the weighted averaged image, LC CXR image, HC CXR image, and the weight value at the corresponding location (i, j), respectively.

The objective is to develop a Convolutional Neural Network (CNN) model that can generate a weight map characterized by values that span the range of 0 to 1. The coefficients of the weight map can be conceptualized as the fusion rule that determines the proportion of each pixel's intensity value from the source image to be utilized during the weighted-average process. The weight value in the weight map is ultimately decided by the probability obtained from the Softmax process. In the proposed network architecture, every branch is equipped with a single max-pooling layer and three convolutional layers. Table 1 displays the suggested CNN's specific parameters. The selection of image patch size is of utmost importance, as there exists an inverse relationship between patch size and categorization performance [24]. The inclusion of larger patch sizes in neural networks has been found to enhance accuracy due to the increased encoding of visual properties. However, it is important to note that this also leads to a significant expansion of the fully-connected layer, which can have implications for computational efficiency.

However, the reliability of the training accuracy diminishes when utilizing small patches. In this study, the utilization of 16 × 16 patches is implemented, considering the aforementioned concerns and the dimensions of the dataset image. The method integrated the 256 feature mappings of each branch into a fully connected 256-dimensional feature vector. The first fully connected layer is then connected to a two-dimensional vector for the purpose of performing the Softmax operation. Ultimately, a 2-way Softmax layer is utilized to process the 2-dimensional vector, resulting in the generation of a probability score that corresponds to the two classes. The complete process of establishing a link may be mathematically modeled as a convolution operation, where the size of the kernel is equivalent to the dimensions of the input image. If the size of the input image is h x b, the weight map can be represented as [ceil (h/ 2) 8 + 1] [ceil (b/ 2) 8 + 1] [25]. The reduction in size of the input image from 8 × 8–16 × 16 is a result of the max-pooling method, which effectively reduces the image dimensions by half. From a conceptual standpoint, convolution, maxpooling, and concatenation can be seen as feature extraction techniques. The pair of image patch pictures is subsequently determined by utilizing probabilistic values ranging from 0 to 1 on completely connected layers.

3.3 Dataset Description

The CT images that have been acquired for evaluation are under-sampled and sourced from the COVID-CT-dataset [26]. The dataset consisted of 349 under-sampled COVID CT scans obtained from a cohort of 216 patients. The available data samples are insufficient to significantly enhance the model's performance. The researchers utilized a substantial dataset, known as SARS-CoV-2 CT-scan [27], which consisted of 1252 samples, in order to address the problem of overfitting. The evaluation of the produced model is conducted through two distinct processes, namely pre-

processing and reconstruction. In the implementation phase, the dataset is partitioned into three subsets: 80% is allocated for training the model, 10% is reserved for testing the model's performance, and the remaining 10% is utilized for model validation. The execution of the suggested study is conducted on the Matlab Simulink platform in order to evaluate the efficacy of the reconstruction model.

4. Result and Discussion

Performance Analysis

This section aims to show the efficacy of the suggested network in the context of super-resolution (SR) picture reconstruction. Moreover, in light of the aforementioned fundamental network configurations, multiple hyperparameters were systematically adjusted in order to attain an optimal balance between network efficacy and computing efficiency.

Performance evaluations play a crucial role as fundamental indicators in the field of image denoising. Throughout the course of time, scholars have employed many objective assessment techniques in the realm of CNN image denoising [28]. Researchers in the field of CNN denoising have employed many evaluation methodologies to assess the performance and effectiveness of their proposed techniques.

a. RMSE

The root mean square error (RMSE) is a commonly employed metric for quantifying the discrepancy between predicted values and the corresponding observed values. The mean squared error (MSE) can be defined as the square of the root mean squared error (RMSE) [29].

$$RMSE = \sqrt{\frac{\sum_{i=1}^{n}(y_i - y_i')^2}{n}} \quad (16)$$

Here n is number of data points. Y_i is actual or observed value for the i^{th} data point. y_i' is predicted value for the i^{th} data point. The obtained RMSE value is shown in Table 2 and figure 6.

Table 2: RMSE values obtained for dataset 1 and dataset 2

	Proposed	DBRCNN	Adaptive VGG	SA CNN
dataset1	0.035	0.039	0.078	0.085
dataset2	0.028	0.029	0.089	0.094

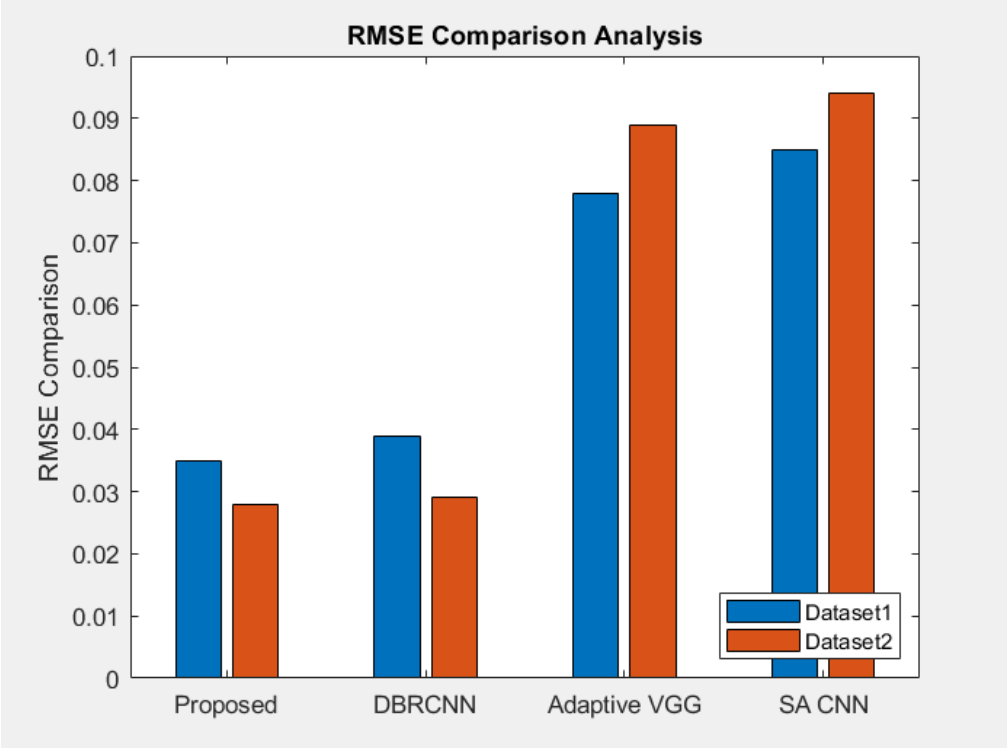

Figure 6: RMSE Comparison between data set 1 and dataset 2

b. PSNR

The Peak Signal-to-Noise Ratio (PSNR) is a widely employed statistic for evaluating the fidelity of reconstructed or compressed pictures. The quantification of image quality is achieved through a comparative analysis between the image in

question and a reference image, often the original image [30]. The equation used to compute the Peak Signal-to-Noise Ratio (PSNR) is given by the following expression:

$$PSNR = 10 \log_{10} \frac{MAX^2}{MSE} \quad (17)$$

Here, MAX is the maximum possible pixel value of the image

MSE is the Mean Squared Error between the original and reconstructed images. The computed PSNR values are given in table 3 and figure 7. In figure 8 the PSNR comparison is shown along with existing methods.

Table 3: Computed values of PSNR for dataset 1 and dataset 2

	Proposed	**DBRCNN**	**Adaptive VGG**	**SACNN**
dataset1	42.3	42.1	41.3	39.6
dataset2	43.1	41.96	41.4	40.98

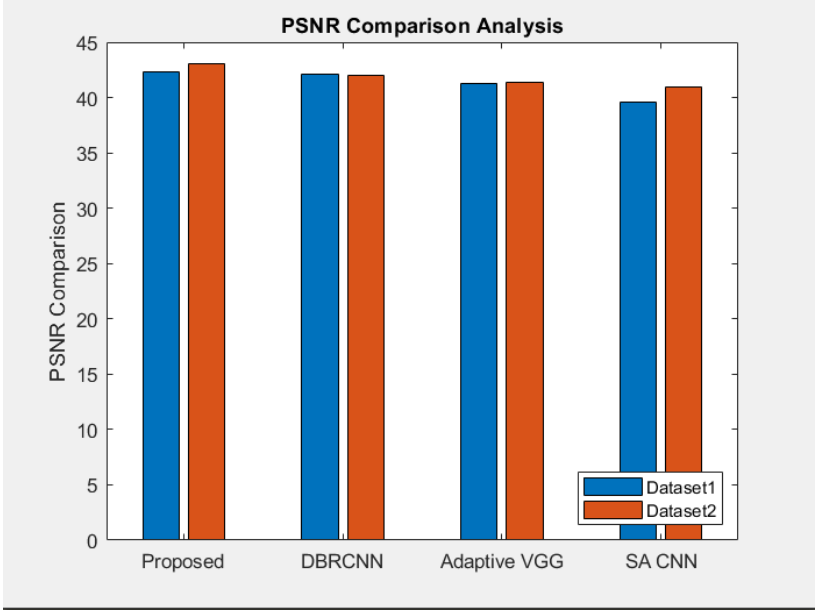

Figure 8: Comparison of PSNR value with proposed and existing method

Table 4: Performance of PSNR at different variance

Variance	**Proposed**	**DBRCNN**	**SRCNN**
0.005	33.04	32.03	31.41
0.02	31.15	30.75	30.22
0.04	26.63	25.19	23.63
0.06	25.85	24.22	20.22
0.08	22.35	21.77	19.33
0.10	21.22	20.12	17.55

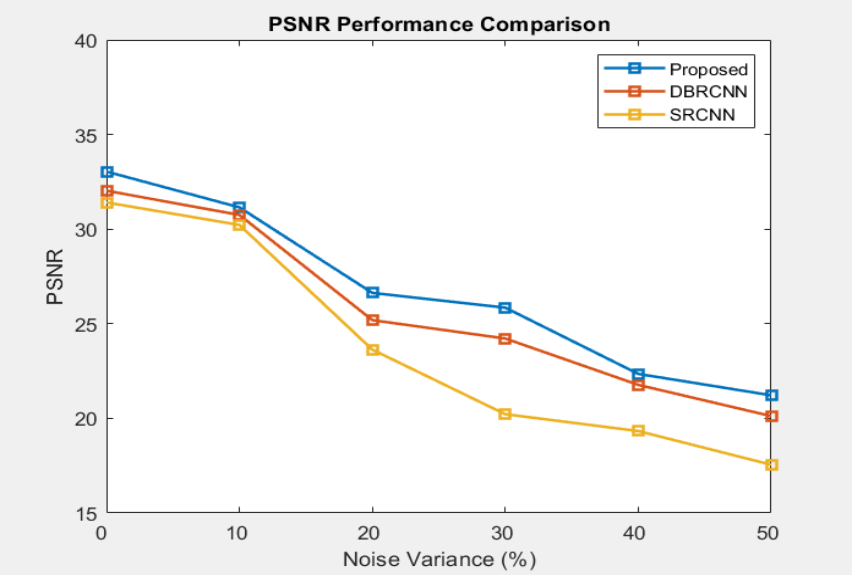

Figure 9: Performance analysis of PSNR

c. SSIM

The Structural resemblance Index (SSI or SSIM) is a quantitative tool employed for assessing the degree of resemblance between two photographs. The full evaluation of image quality takes into account brightness, contrast, and structure, offering a more holistic analysis compared to measurements such as Mean Squared Error (MSE) or Peak Signal-to-Noise Ratio (PSNR). The equation representing the Structural Similarity Index (SSIM) is as follows:

$$SSIM(x,y) = \frac{(2\mu_x\mu_y+c_1)(2\sigma_{xy}+c_2)}{(\mu_x^2+\mu_y^2+c_1)(\sigma_x^2+\sigma_y^2+c_2)} \quad (18)$$

Here x and y are compared images. μ_x and μ_y are means of x and y. σ_x^2 and σ_y^2 are variance of x and y. σ_{xy} is covariance of x and y. c_1 and c_2 are constants to stabilize the division with weak denominator. The obtained SSIM for proposed work is given in table 4 and figure 10 and 11.

Table 5: SSIM with different noise variance

Variance	Proposed	DBRCNN	SRCNN
0.005	0.8761	0.8692	0.8589
0.02	0.8991	0.883	0.8325
0.04	0.8896	0.886	0.766
0.06	0.8751	0.8416	0.6937

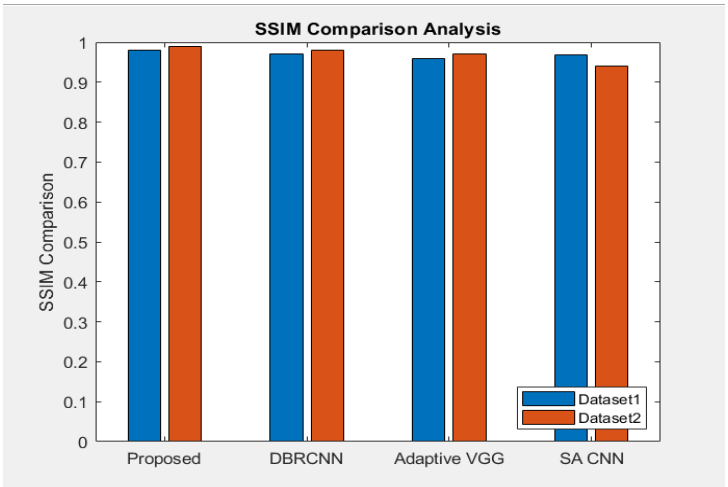

Figure 10: Comparison of SSIM value with proposed and existing method

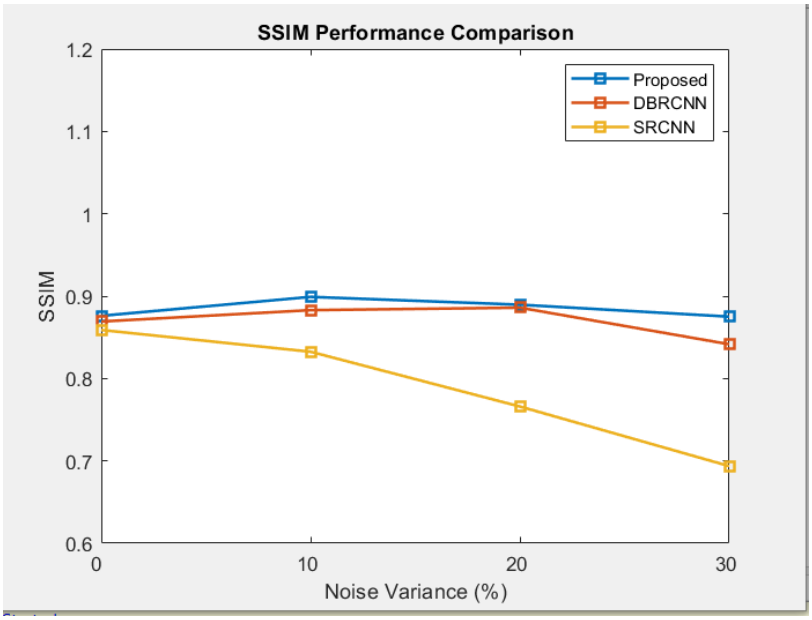

Figure 11: Performance Comparison of SSIM

d. EPI

The EPI quantifies the conserved quantity of edges in the test image. Edges play a crucial role in medical image processing as they contain valuable information. Hence, the Euclidean Performance Index (EPI) between the reference image and the test image can be expressed as follows:

$$EPI(\mu_n, \mu_{original}) = \frac{\Sigma(\Delta\mu_n - \chi_{\Delta\mu_n})(\Delta\mu_{original} - \Delta_{\Delta original})}{\sqrt{\Sigma(\Delta\mu_n - \chi_{\Delta\mu_n})^2 (\Delta\mu_{original} - \Delta_{\Delta original})^2}} \quad (19)$$

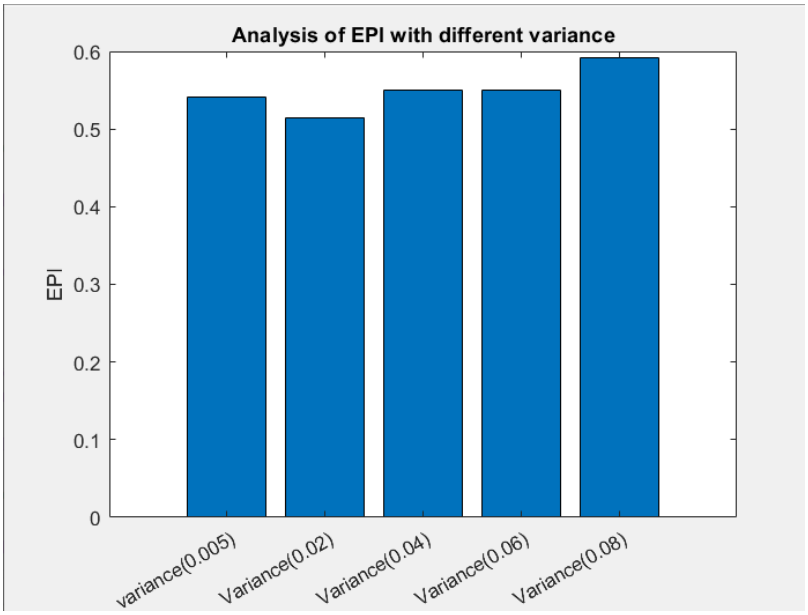

Figure 12: Result comparison of EPI at different variance

e. Over all Analysis of Proposed work

The computation and analysis of picture quality metrics, such as Peak Signal-to-Noise Ratio (PSNR), Structural Similarity Index (SSIM), and Root Mean Square Error (RMSE), are performed using established methodologies. In order to assess the efficacy of the proposed methodology, a comparative analysis is conducted between the DBRCNN, Adaptive VGG, SA CNN models and the aforementioned reconstruction model. The current methodologies have a significantly low peak signal-to-noise ratio (PSNR) and structural similarity index measure (SSIM) as a result of their inferior resolution and elevated reconstruction error. The performance metrics of the planned

work under varying variances are presented in Table 6 and Figure 13.

Table 6: Performance analysis of proposed work

Metrics	Variance (0.005)	Variance (0.02)	Variance (0.04)	Variance (0.06)	Variance (0.08)
RMSE	0.124604	0.2061	0.2662	0.3054	0.332509
EPI	0.54048	0.51502	0.54955	0.55	0.59212
SI	0.53048	0.52502	0.54955	0.5432	0.5822

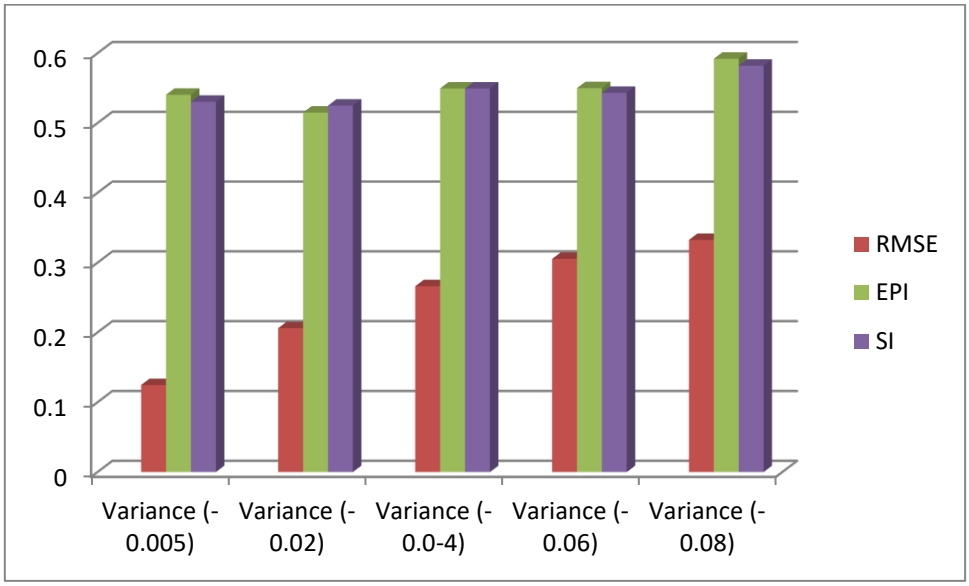

Figure 13: Overall Performance Comparison

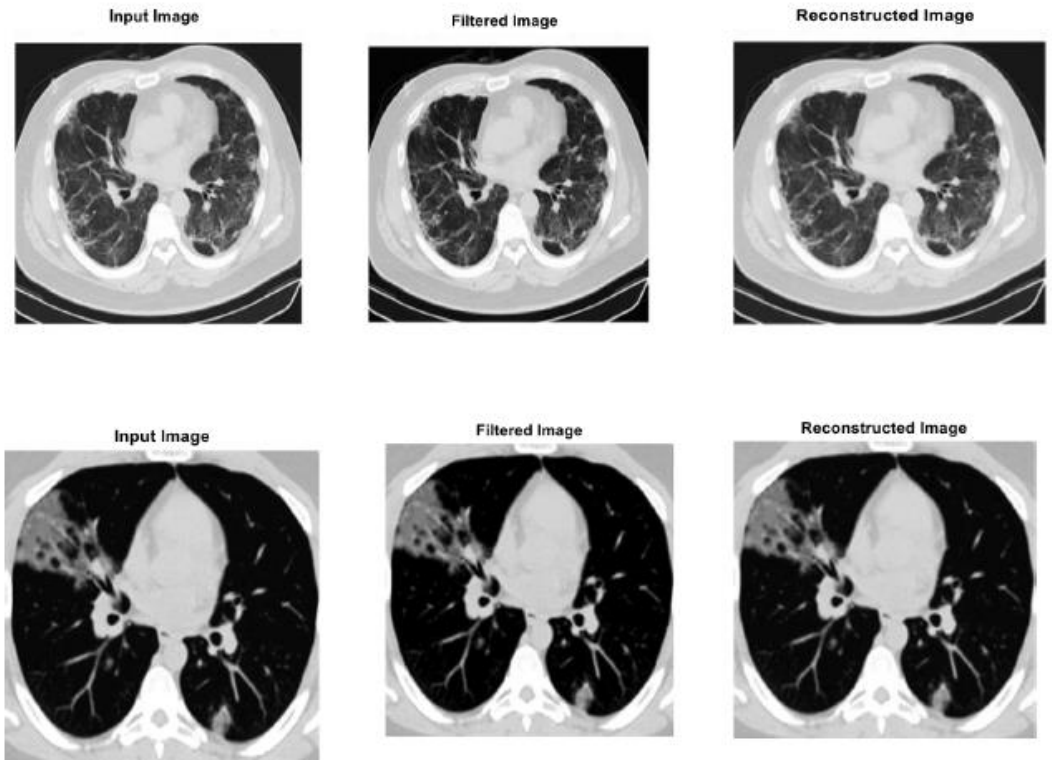

Figure 14: Overall performance of Proposed Work

f. Accuracy and Loss

The suggested model is evaluated using both training and testing datasets. In the analysis of Dataset I, the accuracy and loss curves are evaluated. The dataset was divided such that 80% of the data was allocated for training the model, while the remaining 20% was reserved for testing purposes. Figure 15 depicts the training and testing accuracy of the suggested reconstruction model and which is calculated by using equation (20). The accuracies are evaluated by altering the epoch size. The level of accuracy for both scenarios is comparable. When examining the training and testing accuracy, little fluctuations are detected with a high level of precision. The potential cause for the observed improvement in accuracy can be attributed to the progressive enlargement of the epoch size. When the epoch size is set to 50, the suggested model achieves training, testing, and validation accuracies ranging from 70% to 80% consecutively. When the epoch size is repeatedly increased to 100, 150, and 200, the model consistently maintains an accuracy level ranging from 80% to 90%.

$$Accuracy = \frac{number\ of\ correctly\ classified\ pixels}{total\ number\ of\ Pixels} \quad (20)$$

$$Loss = -iy_i \log(y_i) \quad (21)$$

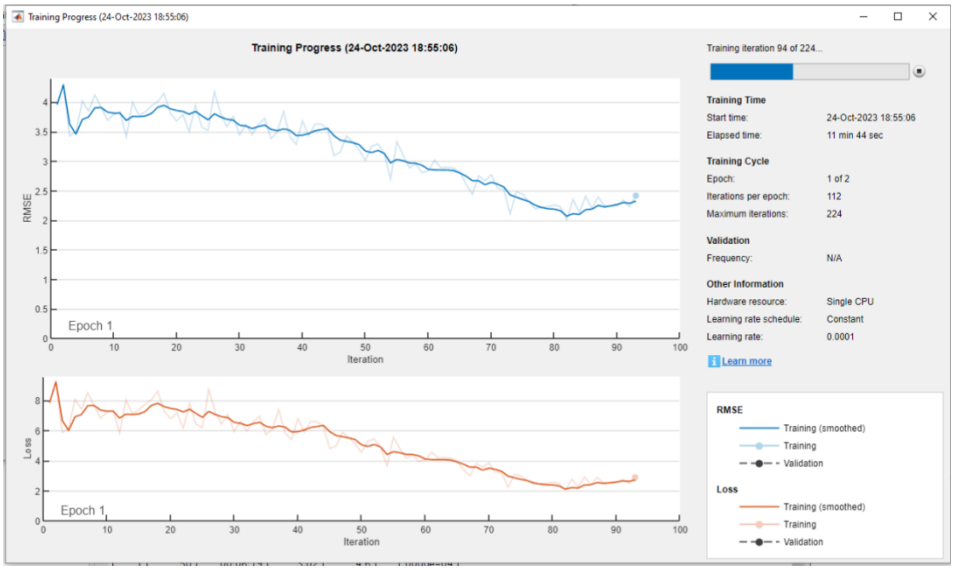

Figure 15: Training, Testing for Accuracy and loss

5. Conclusion

In summary, the importance of medical imaging in contemporary clinics cannot be overemphasized, as it serves as an essential instrument for facilitating diagnoses and providing valuable insights for the development of appropriate treatment approaches. The process of image reconstruction is a fundamental aspect of medical imaging, playing a pivotal role in the acquisition of high-quality medical pictures while minimizing potential risks and costs for patients. This study has traditionally relied on mathematical models that are built by humans and are based on hypotheses. However, in order to enhance the effectiveness of image reconstruction, the study has now explored the utilization of deep learning techniques.

This study demonstrates the potential of artificial intelligence in improving the quality and efficiency of medical image reconstruction by utilizing an Enhanced Convolutional Neural Network (ECNN) in combination with Fuzzy Granular filtering for noise reduction and feature augmentation. The implementation of deep learning methods not only mitigates the laboriousness of manual restoration but also substantially alleviates the computing load associated with the procedure.

Moreover, the incorporation of deep learning, specifically ECNN, exhibits a significant enhancement in precision when contrasted with traditional approaches. This technological progress not only improves the dependability of reconstructed medical images but also facilitates a more efficient and simplified workflow in clinical environments. The ongoing advancement of technology has led to the utilization of deep learning in the field of medical image reconstruction. This development showcases the significant impact that artificial intelligence can

have on healthcare, offering the potential for improved patient care through the convergence of diagnostic accuracy and efficiency.

6. References

[1] Willemink MJ, Noël PB. The evolution of image reconstruction for CT-from filtered back projection to artificial intelligence. Eur Radiol 2019; 29:2185-95.

[2] Goodenberger MH, Wagner-Bartak NA, Gupta S, Liu X, Yap RQ, Sun J, Tamm EP, Jensen CT. Computed Tomography Image Quality Evaluation of a New Iterative Reconstruction Algorithm in the Abdomen (Adaptive Statistical Iterative Reconstruction-V) a Comparison With Model-Based Iterative Reconstruction, Adaptive Statistical Iterative Reconstruction, and Filtered Back Projection Reconstructions. J Comput Assist Tomogr 2018;42:184-90.

[3] Y. Chen, V. Phonevilay, J. Tao et al., "The face image superresolution algorithm based on combined representation learning," Multimedia Tools and Applications, vol. 80, no. 20, pp. 30839–30861, 2021.

[4] Y. Yuan, W. Su, and D. D. Ma, "Efficient dynamic scene deblurring using spatially variant deconvolution network with optical flow guided training," in Proceedings of the 2020 IEEE/ CVF Conference on Computer Vision and Pattern Recognition (CVPR), pp. 13–19, IEEE, Seattle, WA, USA, June 2020.

[5] Po-Yu Liu, "Image Reconstruction Using Deep Learning", https://doi.org/10.1002/9781119861850.ch5, 18 November 2022.

[6] Chun Yang, Wenzhe Wang, Dingye Cui1, Jinliang Zhang, Ling Liu, Yuxin Wang, Wei Li, " Deep learning image reconstruction algorithms in low-dose radiation abdominal computed tomography: assessment of image quality and lesion diagnostic confidence", *Quantitative Imaging in Medicine and Surgery*;13(5):3161-3173 | https://dx.doi.org/10.21037/qims-22-1227, 2023.

[7] Zuozheng Lian , Haizhen Wang , and Qianjun Zhang, "An Image Deblurring Method Using Improved U-Net Model", Hindawi Mobile Information Systems, Volume 2022, Article ID 6394788, 11 pages, https://doi.org/10.1155/2022/6394788.

[8] Akurathi Aravinda, Challagulla Yoshitha, Kakarla Meghana, Kandula Sreeja, B.Tejaswi, " Image Restoration using Deep Learning Techniques", International Journal of Engineering and Advanced Technology (IJEAT) ISSN: 2249-8958 (Online), Volume-11 Issue-5, June 2022.

[9] Kevin De and Yair Rivenson, "Deep-Learning-Based Image Reconstruction and Enhancement in Optical Microscopy", IEEE, DOI: 10.1109/JPROC.2019.2949575, 2023.

[10] Imran Ul Haq, "An Overview Of Deep Learning In Medical Imaging", IEEE Access, 2021.

[11] Muhammad Yaqub , Feng Jinchao , Kaleem Arshid , Shahzad Ahmed ,Wenqian Zhang ,Muhammad Zubair Nawaz , and Tariq Mahmood, "Deep Learning-Based Image Reconstruction for Different Medical Imaging Modalities", Computational and Mathematical Methods in Medicine, Volume 2022, Article ID 8750648, https://doi.org/10.1155/2022/8750648.

[12] Wojciech W, Ewa P. Granular filter in medical image noise suppression and edge preservation. Biocybern Biomed Eng (2018), https://doi.org/10.1016/j.bbe.2018.09.006

[13] Li, P.; Liang, J.; Zhang, M. A degradation model for simultaneous brightness and sharpness enhancement of low-light image. Signal Process. 2021, 189, 108298.

[14] Bai X, Wang X, Liu X, Liu Q, Song J, Sebe N, Kim B. Explainable deep learning for efficient and robust pattern recognition: A survey of recent developments. Pattern Recognit. 2021, 120, 108102.

[15] Padhy, R.P. Chang, X.Choudhury, S.K. Sa, P.K.Bakshi, S. Multi-stage cascaded deconvolution for depth map and surface normal prediction from single image. Pattern Recognit. Lett. 2019, 127, 165–173.

[16] Smith, D.; Gopinath, S. Arockiaraj, F.G. Reddy, A.N.K.; Balasubramani, V. Kumar, R.Dubey, N.Ng, S.H. Katkus, T. Selva, S.J. et al. Nonlinear Reconstruction of Images from Patterns Generated by Deterministic or Random Optical Masks—Concepts and Review of Research. J. Imaging 2022, 8, 174.

[17] Arora, G. Dubey, A.K. Jaffery, Z.A. Rocha, A. A comparative study of fourteen deep learning networks for multi skin lesion classification (MSLC) on unbalanced data. Neural Comput. Appl. 2022, 1, 27.

[18] Yan Wang, Wei Song, Giancarlo Fortino, Li-Zhe Qi, Wenqiang Zhang, Antonio Liotta

[19] An experimental-based review of image enhancement and image restoration methods for

underwater imaging, IEEE Access, 7 (2019), pp. 140233-140251

[20] Yuma Kinoshita, Hitoshi Kiya, "Hue-correction scheme based on constant-hue plane for deep-learning-based color-image enhancement", IEEE Access, 8 (2020), pp. 9540-9550

[21] Dimitris Perdios, Manuel Vonlanthen, Florian Mart inez, Marcel Arditi, Jean-Philippe Thiran CNN-based ultrasound image reconstruction for ultrafast displacement tracking IEEE Trans. Med. Imaging, 40 (3) (2020), pp. 1078-1089.

[22] Anthony DiSpirito, Daiwei Li, Tri Vu, Maomao Ch en, Dong Zhang, Jianwen Luo, Roarke Horstmeyer, Junjie Yao Reconstructing undersampled photoacoustic microscopy images using deep learning IEEE Trans. Med. Imaging, no. 2 (2020), pp. 562-570.

[23] Yanxing Qi, Yi Guo, Yuanyuan Wang, "Image quality enhancement using a deep neural network for plane wave medical ultrasound imaging", IEEE Trans. Ultrason., Ferroelectr., Freq. Control, no. 4 (2020), pp. 926-934

[24] Mehmet Yamac, Mete Ahishali, Aysen Degerli, Ser kan Kiranyaz, Muhammad
E.H. Chowdhury, Moncef Gabbouj Convolutional sparse support estimator-based COVID-19 recognition from X-ray images IEEE Trans. Neural Netw. Learn. Syst. 32, no. 5 (2021), pp. 1810-1820.

[25] Shanjiang Tang, Chunjiang Wang, Jiangtian Nie, N eeraj Kumar, Yang Zhang, Zehui Xiong, Ahmed B arnawi EDL-COVID: ensemble deep learning for COVID-19 case detection from chest x-ray images IEEE Trans. Ind. Inform. 17, no. 9 (2021), pp. 6539-6549

[26] Tawsifur Rahman, Amith Khandakar, Muhammad Abdul Kadir, Khandaker Rejaul Islam, Khandakar F. Islam, Rashid Mazhar, Tahir Hamid, et al. Reliable tuberculosis detection using chest X-ray with deep learning, segmentation and visualization IEEE Access, 8 (2020), pp. 191586-191601.

[27] Seyed Mohammad Jafar Jalali, Milad Ahmadian, Sajad Ahmadian, Ra chid Hedjam, Abbas Khosravi, Saeid Nahavandi X-ray image based COVID-19 detection using evolutionary deep learning approach Expert Syst. Appl. (2022), Article 116942.

[28] Jensen CT, Gupta S, Saleh MM, Liu X, Wong VK, Salem U, Qiao W, Samei E, Wagner-Bartak NA. Reduced-Dose Deep Learning Reconstruction for Abdominal CT of Liver Metastases. Radiology 2022;303:90-8.

[29] J. Pan, "Research progress on deep learning-based image deblurring," Computer Science, vol. 48, no. 3, pp. 9–13, 2021.

[30] H. Yang and Y. Wang, "An effective and comprehensive image super resolution algorithm combined with A novel convolutional neural network and wavelet transform," IEEE Access, vol. 9, pp. 98790–98799, 2021.

[31] Rahul N, Dr. Nagaraj G Cholli , "Image Reconstruction Using Deep Neural Networks Models", International Journal for Research in Applied Science & Engineering Technology (IJRASET), ISSN: 2321-9653; IC Value: 45.98; SJ Impact Factor: 7.538, Volume 10 Issue VIII Aug 2022.